

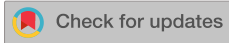


RESEARCH ARTICLE | DECEMBER 24 2015

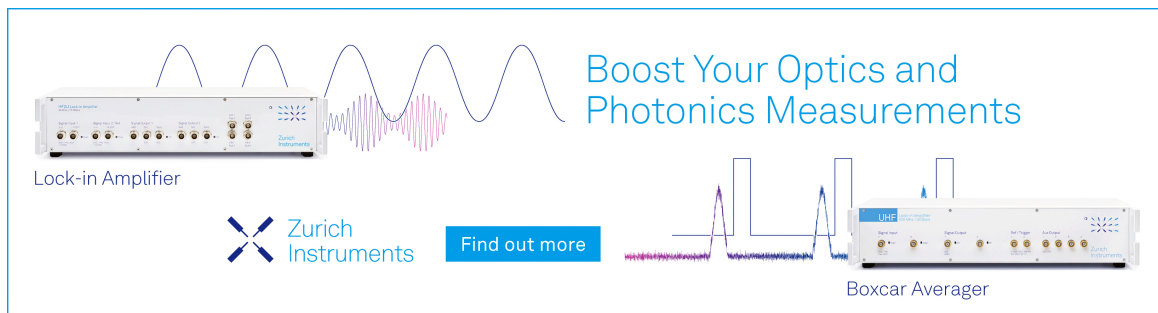
# Compact turnkey focussing neutron guide system for inelastic scattering investigations

G. Brandl; R. Georgii ; S. R. Dunsiger; V. Tsurkan; A. Loidl ; T. Adams; C. Pfeleiderer; P. Böni




*Appl. Phys. Lett.* 107, 253505 (2015)

<https://doi.org/10.1063/1.4938503>



Boost Your Optics and Photonics Measurements

Lock-in Amplifier

 Zurich Instruments

[Find out more](#)

Boxcar Averager

## Compact turnkey focussing neutron guide system for inelastic scattering investigations

G. Brandl,<sup>1,a)</sup> R. Georgii,<sup>2</sup> S. R. Dunsiger,<sup>3</sup> V. Tsurkan,<sup>4</sup> A. Loidl,<sup>5</sup> T. Adams,<sup>6</sup> C. Pfeleiderer,<sup>6</sup> and P. Böni<sup>6</sup>

<sup>1</sup>Heinz Maier-Leibnitz Zentrum (MLZ) and Physik Department E21, Technische Universität München, 85748 Garching, Germany and Jülich Centre for Neutron Science (JCNS) at Heinz Maier-Leibnitz Zentrum (MLZ), Forschungszentrum Jülich GmbH, 85748 Garching, Germany

<sup>2</sup>Heinz Maier-Leibnitz Zentrum (MLZ) and Physik Department E21, Technische Universität München, 85748 Garching, Germany

<sup>3</sup>Physik Department E21, Technische Universität München, 85748 Garching, Germany and Center for Emergent Materials, Ohio State University, Columbus, Ohio 43210-1117, USA

<sup>4</sup>Experimental Physics V, Center for Electronic Correlations and Magnetism, Institute of Physics, University of Augsburg, 86159 Augsburg, Germany and Institute of Applied Physics, Academy of Sciences of Moldova, MD 2028 Chisinau, Republic of Moldova

<sup>5</sup>Experimental Physics V, Center for Electronic Correlations and Magnetism, Institute of Physics, University of Augsburg, 86159 Augsburg, Germany

<sup>6</sup>Physik Department E21, Technische Universität München, 85748 Garching, Germany

(Received 10 November 2015; accepted 10 December 2015; published online 24 December 2015)

We demonstrate the performance of a compact neutron guide module which boosts the intensity in inelastic neutron scattering experiments by approximately a factor of 40. The module consists of two housings containing truly curved elliptic focussing guide elements, positioned before and after the sample. The advantage of the module lies in the ease with which it may be reproducibly mounted on a spectrometer within a few hours, on the same timescale as conventional sample environments. It is particularly well suited for samples with a volume of a few mm<sup>3</sup>, thus enabling the investigation of materials which to date would have been considered prohibitively small or samples exposed to extreme environments, where there are space constraints. We benchmark the excellent performance of the module by measurements of the structural and magnetic excitations in single crystals of model systems. In particular, we report the phonon dispersion in the simple element lead. We also determine the magnon dispersion in the spinel ZnCr<sub>2</sub>Se<sub>4</sub> ( $V = 12.5 \text{ mm}^3$ ), where strong magnetic diffuse scattering at low temperatures evolves into distinct helical order.

© 2015 AIP Publishing LLC. [<http://dx.doi.org/10.1063/1.4938503>]

Inelastic neutron scattering from single crystals using triple-axis or time-of-flight spectroscopy is an extremely powerful technique for studying excitations in condensed matter systems, often on energy scales inaccessible via other methods. However, due to the weak nature of the interaction between the neutron and the material of interest, typically large samples of roughly 1 cm<sup>3</sup> are required. The ever increasing complexity of the compounds makes sample size a big concern, as it is often difficult to produce large homogeneous single crystals. An additional restriction may be imposed by extreme sample environments such as pressure or magnetic fields, which can often only be applied to small sample volumes. To overcome the resulting small scattering intensity, it is very important to enhance the flux at the sample position and decrease the background to maintain an acceptable signal to noise ratio.

In conventional triple-axis spectroscopy, the flux at the sample is enhanced by using doubly focussing monochromators and analyzers.<sup>1–3</sup> Here, the beam is focussed by a large number of mosaic crystals yielding a beam of typically 20 × 20 mm<sup>2</sup> at the sample position, limited by the size of the individual monochromator crystals. However, for small samples of a few mm<sup>3</sup> and under extreme conditions, the signal

to noise ratio of the scattered neutrons is reduced due to scattering from the sample environment. Even when using apertures, the neighbourhood of the sample is usually illuminated by the penumbra of the beam.

The use of neutron guides is now widespread. Major developments include the use of supermirror guides,<sup>4</sup> the virtual source concept,<sup>5</sup> or the aforementioned focussing monochromator and analyser arrays. However, these systems are typically intended as semipermanent installations. In this letter, we report the application of a cost effective *turnkey* focussing guide module, which may be reliably installed within hours, tailoring the neutron optics to the experiment at hand for inelastic neutron scattering investigations (Fig. 1(a)). It has been previously applied by Adams *et al.* for neutron diffraction studies of small single crystals.<sup>6</sup> The module consists of two support arms moving on a flat table (GT) around their center of rotation, where the sample (S) is located. On each support arm, a housing (H1, H2) can be placed wherein a focussing guide element (G1, G2) is aligned. The incoming arm is fixed to accept the neutrons from the monochromator (M), while the outgoing arm collects the scattered neutrons guiding them via the analyzer (A) to the detector (D).

The initial alignment of the guides is accomplished optically, adjusting set screws at each end of the guide housings.

<sup>a)</sup>g.brandl@fz-juelich.de

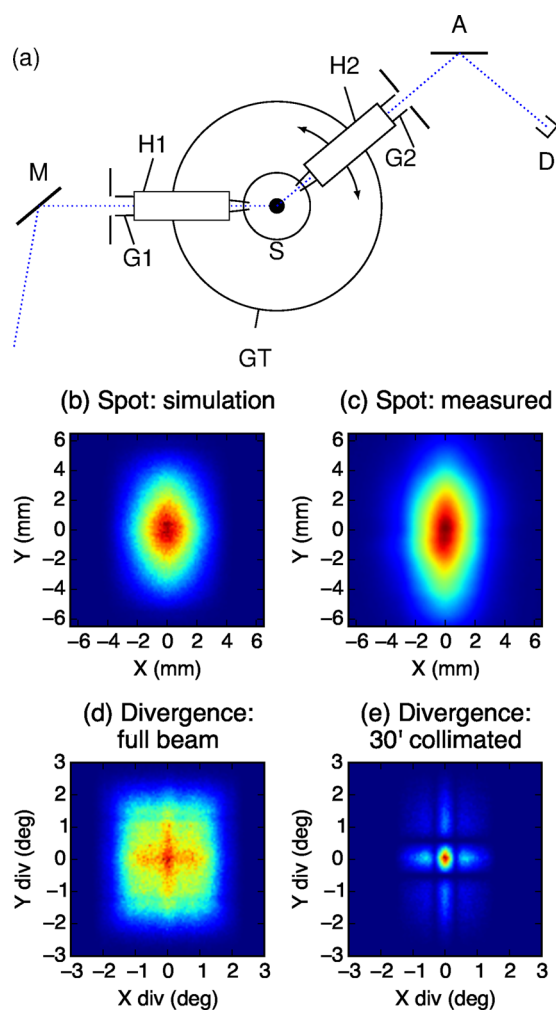


FIG. 1. (a) Schematic of the guide system: two support arms moving on a flat table (GT) around the sample (S). On each support arm, housings (H1, H2) are placed containing focussing guide elements (G1, G2). The two arms are aligned towards the monochromator (M) and analyzer (A), respectively. (b) Simulation of the focal spot with McStas. The FWHM of the spot when fitted with a Gaussian profile is  $3.8 \times 5.9 \text{ mm}^2$  (horizontal  $\times$  vertical). (c) Image of the focal spot made with the neutron camera. The measured FWHM is  $3.6 \times 7.1 \text{ mm}^2$ . Divergence of neutrons in a  $20 \times 20 \text{ mm}^2$  area around the focal spot, (d) with the full incoming divergence of the instrument illuminating the guide entry, and (e) with the incoming divergence illuminating the guide entry restricted to  $30^\circ$ .

It only needs to be done once per housing and forms part of the initial alignment of the spectrometer. Subsequently, using kinematic mounts, the housings containing the aligned guides can be reproducibly removed and replaced during an experiment within minutes. A detailed description of the kinematic mounts and the procedure of alignment, including a discussion of spurious artifacts caused by improper alignment, is given by Adams *et al.*<sup>6</sup>

The experiments described in the following were performed on MIRA<sup>7</sup> at the FRM-II in the triple axis mode of operation, using cold neutrons with a fixed incident wave-number  $k_i = 1.4 \text{ \AA}^{-1}$  ( $\lambda \approx 4.5 \text{ \AA}$ ). Due to the constraints of the instrument, an operation in the constant- $k_f$  mode was not possible. The neutron optics for the whole spectrometer plus guides integrated system must be considered: The monochromator and analyser arrays (both pyrolytic graphite) were flat. The distance between the monochromator and guide entrance was 0.5 m.

The two identical focussing elements G1 and G2 are part of the elliptic guide, which was used previously for diffraction experiments.<sup>6,8</sup> The elements are one quarter of a full elliptic guide and are 500 mm long, while the two ends have the dimensions  $18 \times 9 \text{ mm}^2$  and  $8 \times 4 \text{ mm}^2$ , respectively. To reduce the complexity of the setup, neither the guides nor the housings were evacuated to reduce air scattering. The inner sides are coated with a supermirror with critical angle  $m = 3$  times that of nickel. This sets an upper limit for the incident and final neutron energies at about 10 meV. The focal length as measured from the guide exit was 80 mm. While an ideal full elliptic geometry may be used to create point like sources,<sup>9</sup> the shortened length described adequately approximates a parabolic focussing geometry and is much more compact. Nonetheless, by Liouville's theorem, the phase space volume of the neutron trajectories must be conserved, leading to a more highly divergent beam.

To characterize the beam at the sample position, its profile was measured with DELcam, a high-resolution neutron camera developed at the FRM-II.<sup>10</sup> The measured profile with a full-width at half-maximum (FWHM) of  $3.6 \times 7.1 \text{ mm}^2$  (horizontal  $\times$  vertical (Fig. 1(c)) is reasonably well reproduced by simulations using the Monte-Carlo simulation package McStas,<sup>11</sup> yielding  $3.8 \times 5.9 \text{ mm}^2$  (Fig. 1(b)). The difference can be attributed to the different coatings at the sides ( $m = 1.2$ ) and the top/bottom ( $m = 2.0$ ) of the neutron beamline guide NL6, which was not considered in the simulation. The inhomogeneous divergence distribution at the sample due to the short length of the guides<sup>12</sup> can be reduced by allowing more incoming divergence at the guide entry (Figs. 1(d) and 1(e)). In comparison to the study of Adams *et al.*,<sup>6</sup> the entry of the first guide was placed much closer to the monochromator to take advantage of this effect.

With the guides aligned and reproducibly mounted, we set up the test sample, namely, a lead crystal of cubic shape with the dimensions  $2 \times 2 \times 2 \text{ mm}^3$ , oriented in the (*hhl*) plane. Lead was chosen due to its simple phonon spectrum and relatively large lattice constant ( $4.95 \text{ \AA}$ ). Thus, sufficiently large scattering angles could be attained to access nuclear Bragg positions. A comparison of rocking scans measured at the (002) and (111) Bragg reflections demonstrated an increase in width by a factor of two and of the integrated intensity by a factor of three when compared with the configuration without guides. The shape of the peaks was still largely Gaussian. The gain for diffraction is expected to be low because the Bragg condition restricts the accepted divergence of the beam massively, essentially acting to collimate the beam. No such constraint limits the gain observed inelastically.

The measurements of transverse phonons around the (200) and (111) zone centers (Figs. 2(a)–2(c)) demonstrate a massive increase in the inelastically scattered neutrons of up to a factor of  $G \approx 30 - 40$ , while the background increases only by a factor of 2–5. Therefore, the signal-to-noise ratio increases by a factor of 6–20. In future experiments, the increased background will be addressed systematically, e.g., by better shielding of the immediate environment of the guides, although it is expected that a large fraction of the background originates from the sample itself, while the background produced by the sample environment is decreased

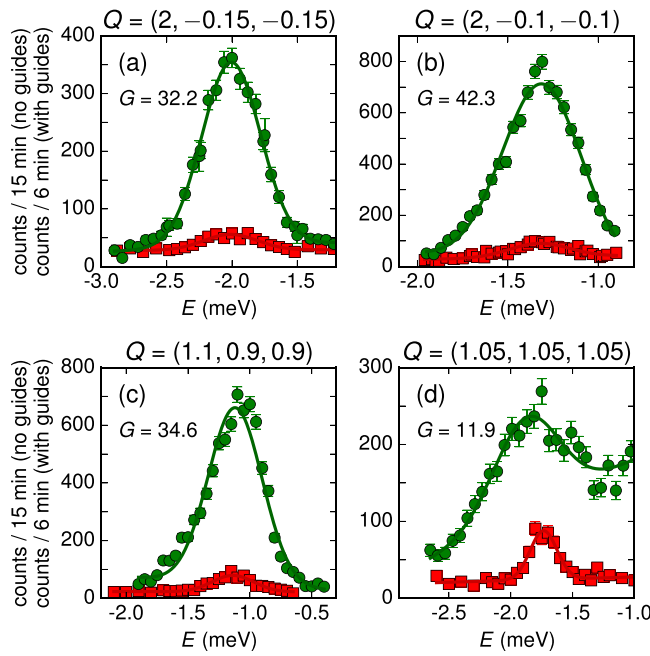


FIG. 2. Comparison of the inelastic scattering from transverse and longitudinal acoustic phonons in lead with (green circles) and without (red squares) guides. The gain factor  $G$  (comparing the integrated intensities of the peaks) is noted for each  $Q$  point. The number of counts for the configuration without guides has been multiplied by 2.5 for better visibility. Note the efficient focussing for transverse phonons.

due to the focussing of the beam. The intensity gains at the detector result from the focussing of the incident neutron beam onto the sample and from the improved collection of the scattered neutrons by the second guide. A 15-fold gain of neutron flux at the sample position agrees with the McStas simulations performed for the sample size investigated. The observed gains are also consistent with McStas simulations of a parabolic  $m = 3$  guide.<sup>13,14</sup> All constant  $Q$ -scans were performed at room temperature on the neutron energy gain side. In order to collect enough statistics for the measurements without focussing, the measurement time was increased from 6 to 30 min per point. The observed phonon energies (see Table I) are consistent with the measurements of Stedman *et al.*<sup>15</sup> and Furrer and Halg,<sup>16</sup> considering the temperature dependence of the phonon frequencies.

Although the intensity for longitudinal acoustic phonons is also increased when using the focussing guides, the spectrum is distorted (Fig. 2(d)). The reason is that the increased divergence of the incident neutrons and the increased angle of acceptance for the scattered neutrons lead to a very coarse  $Q$ -resolution along  $Q$  and therefore to a sampling of phonons

TABLE I. Results of the transverse phonon measurements in lead in the  $(0kk)$  and  $(kkk)$  directions.

$Q$	$E, \Gamma$ (meV)		Gain
	Guides	No guides	
(1.1, 0.9, 0.9)	-1.14, 0.10	-1.12, 0.13	35
(2, -0.1, -0.1)	-1.31, 0.13	-1.33, 0.10	42
(2, -0.15, -0.15)	-2.01, 0.12	-2.01, 0.13	32
(2, -0.3, -0.3)	-3.87, 0.21	n.a.	n.a.
(2, -0.5, -0.5)	-6.61, 0.19	n.a.	n.a.

over an extended range  $\Delta Q$ . In contrast, the  $Q$ -resolution relevant for transverse phonons, i.e., perpendicular to  $Q$ , is essentially unaffected.

The large gain factors for transverse phonons were reproduced at other  $Q$ -positions as well. The system turned out to be essential, in particular, for phonons at higher energies, which could not otherwise be measured without the focussing guides. It is obvious that the focussing guides will be most effective for measurements of optic phonons and phonons near the zone boundary when the dispersion becomes flat and the  $Q$ -resolution along  $Q$  becomes irrelevant.

Finally, we demonstrate the power of the focussing configuration for the determination of the magnon spectrum of the spinel  $\text{ZnCr}_2\text{Se}_4$ , a system where the limited size of the available single crystals has prohibited inelastic neutron scattering investigations till date. This compound is one of a rich series with the composition  $A\text{Cr}_2X_4$  ( $X = \text{O}, \text{S}, \text{Se}$  and  $A = \text{Zn}, \text{Mg}, \text{Cd}, \text{Hg}$ ), where the arrangement of the ( $S = 3/2$ ) Cr ions on a pyrochlore lattice or network of corner sharing tetrahedra can in some cases lead to magnetic geometric frustration.<sup>17</sup> The frustration is further enhanced by the presence of competing antiferromagnetic and ferromagnetic (FM) exchange and superexchange paths. As a function of lattice constant, or equivalently as a function of Cr–Cr separation, these compounds are characterized by Curie–Weiss (CW) temperatures from  $-400$  to  $200$  K and, at low temperatures, reveal either complex antiferromagnetism or ferromagnetism.<sup>18</sup> In the case of  $\text{ZnCr}_2\text{Se}_4$ , which is dominated by strong FM interactions (evidenced by a Curie–Weiss temperature of  $90$  K), a number of elastic neutron scattering studies have been carried out to determine the magnetic structure.<sup>19,20</sup> As the temperature is reduced,  $\text{ZnCr}_2\text{Se}_4$  develops strong diffuse scattering around  $(\delta, 0, 0)$  with  $\delta = 0.44$  and finally undergoes a transition to an incommensurate AFM helix state at  $T_N = 21$  K, with a FM arrangement in the  $(100)$  planes and a turning angle of  $42^\circ$  between planes. The ordered moment of the Cr ions is  $1.9\mu_B$  at low temperature.<sup>20</sup> The compound  $\text{ZnCr}_2\text{Se}_4$  offers several advantages: the magnetic ordering is incommensurate, and thus, any magnetic signal is clearly separated from nuclear scattering. In addition, the prevalence of diffuse scattering implies that fine  $Q$  resolution is unnecessary, and finally, the presence of FM correlations allows us to examine the response around the main beam near “forward scattering,” taking advantage of the magnetic form factor.

The single crystal was prepared by solid-state reaction from high purity elements in evacuated quartz ampoules. The cuboidal sample shape has dimensions of  $2 \times 2.5 \times 2.5 \text{ mm}^3$ . It was mounted in an  $(hll)$ -plane, and scans were conducted at the transverse  $Q$ -positions  $(0.44, l, l)$  using neutrons with a constant  $k_i = 1.22 \text{ \AA}^{-1}$  and the focussing setup. Shown in Fig. 3 are some of the resulting spectra at  $3.5$  K. A single dispersing excitation is visible, which becomes quickly broader with increasing  $q$ , where  $q$  is measured with respect to the  $(0.44, 0, 0)$  peak of the helix. Similar scans taken at  $T = 60$  K, well above the regime of diffuse scattering, do not show any well defined excitation peaks.

To extract a magnon dispersion, we fitted the scans with a damped harmonic oscillator function of the form

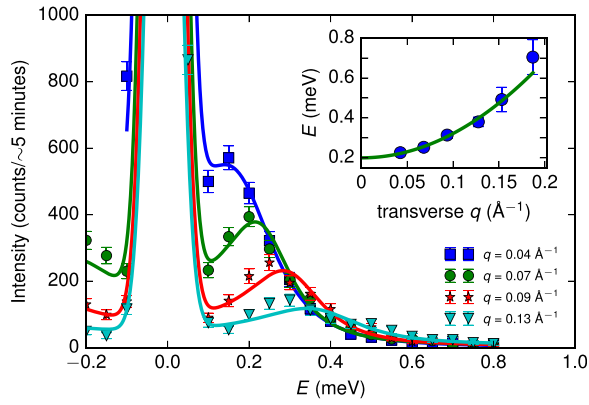


FIG. 3. Inelastic constant- $Q$  scans of  $\text{ZnCr}_2\text{Se}_4$  measured at  $T = 3.5$  K at different transverse  $Q$  positions relative to the magnetic Bragg peak (0.44, 0, 0). The inset shows the energy position of the excitations extracted from the spectra, when fitted with the model of a damped harmonic oscillator. The green line shows the best fit for the assumed dispersion relation  $E_q = \Delta + Dq^2$ , with  $\Delta = 0.2$  meV and  $D = 8.8$  meVÅ<sup>2</sup>.

$$S(q, E) = I_0 \langle n(E) \rangle \frac{\Gamma}{(E_q^2 - E^2)^2 + \Gamma^2 E^2}$$

Here,  $I_0$  is a normalization constant,  $\Gamma$  the linewidth of the excitation, and  $\langle n(E) \rangle$  the Bose factor for annihilation. The incoherent scattering at  $E = 0$  was taken into account by adding a Gaussian with a FWHM representing the instrumental energy resolution of  $76 \mu\text{eV}$  at the elastic line, determined from the incoherent scattering of vanadium. Note that in the absence of the focussing guides, the energy resolution found using vanadium was the same.

The magnon energies follow a quadratic dispersion relation  $E_q = \Delta + Dq^2$ , as shown in the inset of Fig. 3, with an energy gap  $\Delta = 0.2$  meV and  $D = 8.8$  meVÅ<sup>2</sup>. The latter depends on the strength of the exchange interactions and is proportional to the magnetic ordering temperature. These results clearly demonstrate the dominance of the ferromagnetic exchange and provide the energy scale of the ferromagnetic coupling. Note that previous experiments without using focussing guides did not have sufficient neutron flux at the sample to distinguish any inelastic scattering from the instrumental background. A detailed description of the magnetic response of  $\text{ZnCr}_2\text{Se}_4$  will appear elsewhere.

In conclusion, we have developed a compact neutron guide module for inelastic neutron scattering, which can be quickly installed at existing beamlines, allowing the measurement of excitations and diffusion processes from samples with a size of a few mm<sup>3</sup>. It is straightforward to achieve gains in intensity of the order of 40. Using more advanced supermirrors with  $m$ -values of the order of 8 will increase the gains even further and make focussing techniques applicable for neutrons with much lower wavelengths down to 1 Å.<sup>21,22</sup> Most beneficial will be the use of the

focussing module in combination with extreme sample environments, such as pressure cells, where the background can be massively reduced while increasing the signal from the sample. Alternatively, together with polarizing guide coatings, studies with polarized neutrons are possible without the need for additional polarizers. In combination with the miniaturized SNP (Spherical Neutron Polarimetry) device developed by Kindervater *et al.*,<sup>23</sup> this could be a powerful tool for polarized neutron studies on small samples. This cost-effective technique allowed us to probe the excitations in a  $\sim 70$  mg magnetic system with a modest spin only magnetic moment of  $3.87\mu_B$  in the paramagnetic state. It establishes proof of principle and opens up a broad range of scientific investigations using a  $Q$  resolved probe.

This work was partly supported by the Transregional Collaborative Research Center TRR 80 from Electronic Correlations to Functionality (Augsburg, Munich, Stuttgart). We gratefully acknowledge the support by R. Schwikowski, A. Mantwill, and the team of FRM II. Many thanks to J. Neuhaus for helpful discussions and support.

- <sup>1</sup>R. Scherm, G. Dolling, R. Ritter, E. Schedler, W. Teuchert, and V. Wagner, *Nucl. Instrum. Methods* **143**, 77 (1977).
- <sup>2</sup>T. Riste and K. Otnes, *Nucl. Instrum. Methods* **75**, 197 (1969).
- <sup>3</sup>W. Bührer, *Nucl. Instrum. Methods A* **338**, 44 (1994).
- <sup>4</sup>W. Wagner, G. S. Bauer, J. Duppich, S. Janssen, E. Lehmann, M. Lüthy, and H. Spitzer, *J. Neutron Res.* **6**, 249 (1998).
- <sup>5</sup>L. Pintschovius, *Nucl. Instrum. Methods A* **338**, 136 (1994).
- <sup>6</sup>T. Adams, G. Brandl, A. Chacon, J. N. Wagner, M. Rahn, S. Mühlbauer, R. Georgii, C. Pfeleiderer, and P. Böni, *Appl. Phys. Lett.* **105**, 123505 (2014).
- <sup>7</sup>R. Georgii and K. Seemann, *J. Large-Scale Res. Facil. (JLSRF)* **1**, A3 (2015).
- <sup>8</sup>S. Mühlbauer, P. Niklowitz, M. Stadlbauer, R. Georgii, P. Link, J. Stahn, and P. Böni, *Nucl. Instrum. Methods A* **586**, 77 (2008).
- <sup>9</sup>C. Schanzer, P. Böni, U. Filges, and T. Hils, *Nucl. Instrum. Methods A* **529**, 63 (2004).
- <sup>10</sup>M. Mühlbauer, Ph.D. thesis, Technische Universität München, 2013.
- <sup>11</sup>P. Willendrup, E. Farhi, and K. Lefmann, *Physica B* **350**, E735 (2004).
- <sup>12</sup>P. Böni, *J. Phys.: Conf. Ser.* **502**, 012047 (2014).
- <sup>13</sup>T. Hils, P. Böni, and J. Stahn, *Physica B* **350**, 166 (2004).
- <sup>14</sup>N. Kardjilov, P. Böni, A. Hilger, M. Strobl, and W. Treimer, *Nucl. Instrum. Methods A* **542**, 248 (2005).
- <sup>15</sup>R. Stedman, L. Almqvist, and G. Nilsson, *Phys. Rev.* **162**, 549 (1967).
- <sup>16</sup>A. Furrer and W. Hälgl, *Phys. Status Solidi (B)* **42**, 821 (1970).
- <sup>17</sup>T. Rudolf, C. Kant, F. Mayr, J. Hemberger, V. Tsurkan, and A. Loidl, *New J. Phys.* **9**, 76 (2007).
- <sup>18</sup>P. K. Baltzer, P. J. Wojtowicz, M. Robbins, and E. Lopatin, *Phys. Rev.* **151**, 367 (1966).
- <sup>19</sup>R. Plumier, *J. Appl. Phys.* **37**, 964 (1966).
- <sup>20</sup>F. Yokaichiya, A. Krimmel, V. Tsurkan, I. Margiolaki, P. Thompson, H. N. Bordallo, A. Buchsteiner, N. Stüßer, D. N. Argyriou, and A. Loidl, *Phys. Rev. B* **79**, 064423 (2009).
- <sup>21</sup>See <http://www.swissneutronics.ch/index.php?id=24> for an overview of currently available supermirror coatings, 2015.
- <sup>22</sup>C. Schanzer, "Neutron Optics: Towards Applications for Hot Neutrons," *J. Phys: Conf. Ser.* (submitted).
- <sup>23</sup>J. Kindervater, W. Häußler, M. Janoschek, C. Pfeleiderer, P. Böni, and M. Garst, *Phys. Rev. B* **89**, 180408(R) (2014).